Annulenes

DOI: 10.1002/ange.201202324

A Tetrathiafulvalene-Functionalized Radiaannulene with Multiple Redox States**

*Kasper Lincke, Anders Floor Frellsen, Christian Richard Parker, Andrew D. Bond, Ole Hammerich, and Mogens Brøndsted Nielsen**

Radiaannulenes (RAs) are cyclic molecules having both exo- and endocyclic double bonds,[1] and therefore structurally lie between radialenes[2] and annulenes.[3] As they possess a quinoid-like structure (Figure 1), we decided to investigate the possibility for employing them as Wurster-type[4] two-stage redox systems. A benzannelated derivative of octadehydro[14]annulene (**1**) has previously been shown to exhibit 14π aromaticity as asserted from a diatropic ring current.[5] This same core could formally be generated from the expanded RA **2** by reduction. Herein, we have combined **2** with tetrathiafulvalene (TTF, Figure 1), a two-stage Weitz-type[4] redox system which has found wide interest in materials and supramolecular chemistry.[6] By undergoing two one-electron oxidations, TTF achieves two 6π-aromatic 1,3-dithiolium rings,[7] and fusing a TTF unit to each of the endocyclic double bonds of **2** should thus provide a TTF/RA molecule that could potentially exist in seven or more redox states. Each of these are expected to exhibit characteristic electronic excitations in the UV/Vis region and maybe even in the NIR/IR region. Molecules reversibly changing color upon charging/decharging are particularly attractive for the development of electrochromic materials.

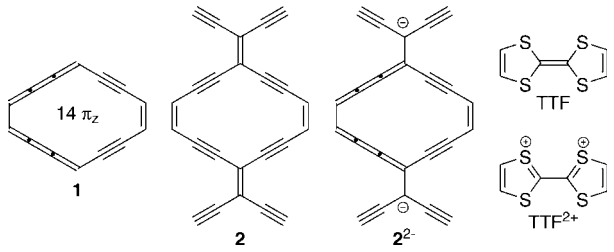

Figure 1. Structures of **1**, **2**, and TTF.

Subjecting the tetraethynylethene (TEE) **3**[8] (after desilylation) and the diiodo TTF **4**[9] to fourfold Sonogashira couplings gave the TTF/RA **5** in a yield of 10%, thus corresponding to 56% yield for each step in the cyclization (Scheme 1). The compound was dark-green in solution and as crystals, but was red when isolated as a solid film. The structure was confirmed by X-ray crystallographic analysis (Figure 2),[10] which showed some bending of the TTF units and triisopropylsilylethynyl groups away from the almost planar RA core.

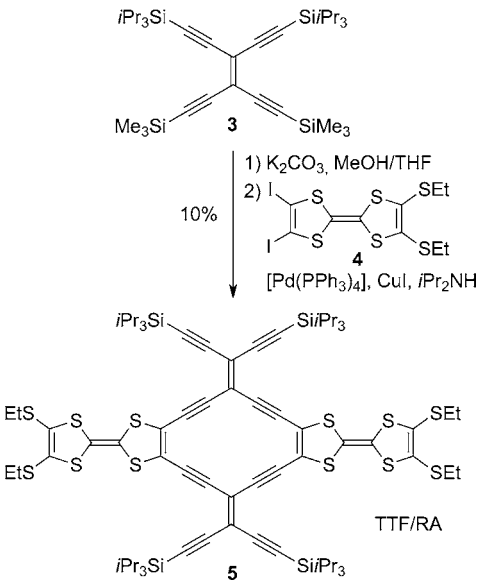

Scheme 1. Synthesis of TTF/RA scaffold. THF = tetrahydrofuran.

Compound **5** comprises two TEE units, which are themselves known to be electron acceptors.[11] For a comparison of properties, we also prepared the related TTF/TEE **6**[9] (Figure 3).

Both **5** and **6** are strong chromophores with broad charge-transfer (CT) transitions in CH_2Cl_2 at approximately $\lambda = 644$ and 522 nm, respectively (Figure 4). This band extended to $\lambda = 800$ nm in the case of **5**, thus suggesting a particularly strong acceptor character of the RA core. The CT character of the absorption was supported by DFT calculations (B3LYP/6-31G(d) using Gaussian 09[12]) on the related molecule **5**(4H) with the silyl groups replaced by H atoms. The HOMO and HOMO−1 reside mainly on the two TTFs (and partially on the external diethynylethenes), while the LUMO resides mainly on the cyclic core (Figure 5).

[*] Dr. K. Lincke, A. Floor Frellsen, Dr. C. R. Parker, Prof. Dr. O. Hammerich, Prof. Dr. M. Brøndsted Nielsen
Department of Chemistry, University of Copenhagen
Universitetsparken 5, 2100 Copenhagen Ø (Denmark)
E-mail: mbn@kiku.dk
Prof. Dr. A. D. Bond
Department of Physics, Chemistry and Pharmacy
University of Southern Denmark, 5230 Odense M (Denmark)

[**] The Danish Council for Independent Research / Natural Sciences (no. 10-082088), The Carlsberg Foundation, and the European Union 7th Framework Programme (FP7/2007–2013) under the grant agreement no. 270369 ("ELFOS") are acknowledged.

Supporting information for this article is available on the WWW under http://dx.doi.org/10.1002/anie.201202324.

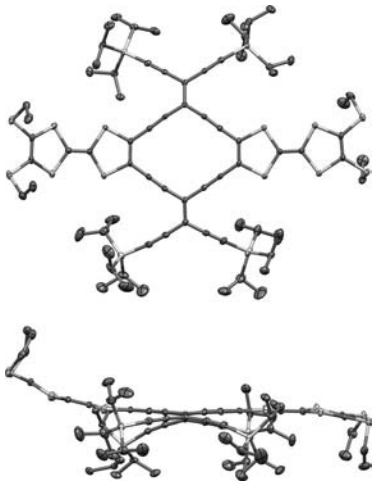

Figure 2. Molecular structure of **5** (H atoms omitted). Displacements ellipsoids shown at 50% probability for non-H atoms. Crystals grown from CH_2Cl_2/MeOH.

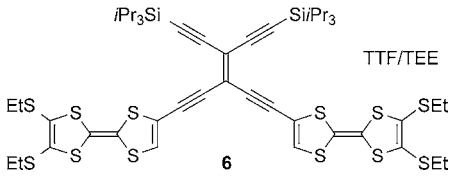

Figure 3. Structure of **6**.

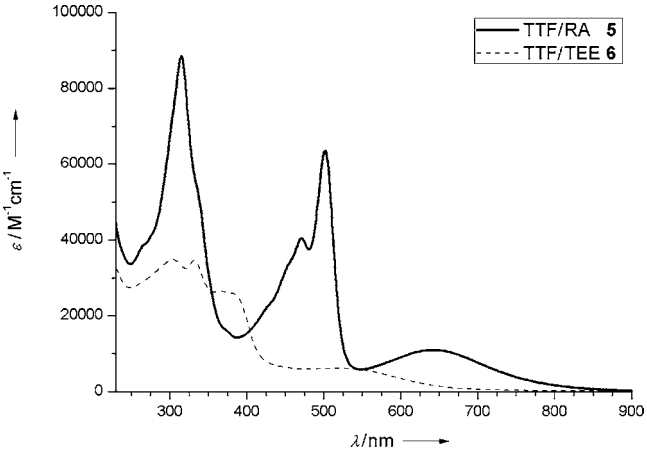

Figure 4. UV/Vis absorption spectra of **5** and **6** in CH_2Cl_2.

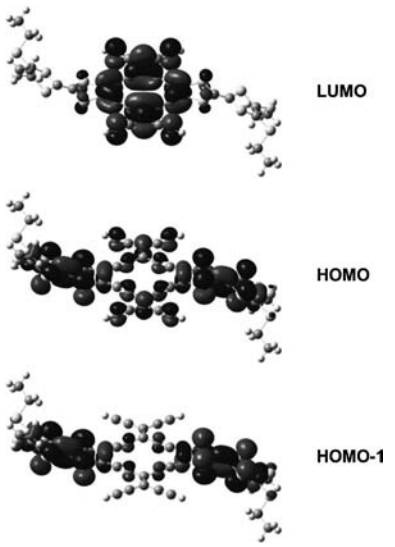

Figure 5. Frontier orbitals of **5**(4 H).

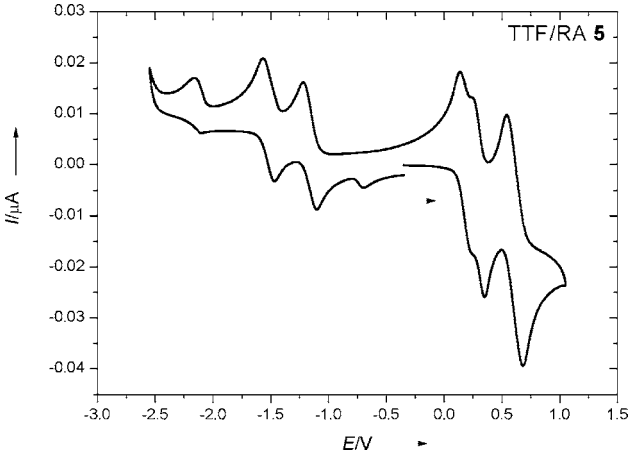

Figure 6. Cyclic voltammogram of **5** in $CH_2Cl_2 + 0.1$ M $[NBu_4][PF_6]$. Scan rate 0.1 Vs^{-1}. Potentials vs $FeCp_2^+/FeCp_2$ as external reference.

TTF/TEE **6** exhibits two reversible two-electron oxidations at $E_{1/2} = +0.12$ and $+0.52$ V vs $FeCp_2^+/FeCp_2$, and the two TTF units are independent redox centers. In contrast, the CV of the TTF/RA **5** (Figure 6) revealed a small splitting of the first oxidation wave into two one-electron oxidations at $E_{1/2} = +0.20$ and $+0.29$ V ($\Delta E_{1/2} = 0.09$ V), thus implying that the two TTFs are oxidized to radical cations sequentially. The first oxidation generates a mixed-valence state as ascertained spectroscopically (see below; Class II compound under the Robin-Day classification system).[13] In a third two-electron oxidation ($+0.61$ V), the tetracation $\mathbf{5}^{4+}$ is generated. Moreover, **5** shows two electrochemically reversible one-electron reductions at $E_{1/2} = -1.16$ V and -1.52 V corresponding to the formation of $\mathbf{5}^-$ and $\mathbf{5}^{2-}$, respectively, and even a third reduction peak is observed close to -2.16 V. Thus, it appears that **5** is considerably easier to reduce than **6** (-1.70 V). Peaks corresponding to the back-oxidation of $\mathbf{5}^{2-}$ and $\mathbf{5}^-$ are seen during the reverse scan together with a minor oxidation peak at -0.70 V. The latter is most likely caused by the oxidation of a monoanion resulting from partial protonation of $\mathbf{5}^{2-}$, probably by residual water. Similar electrochemical behavior has been observed in other cases.[14]

The different charge states of **5** are characterized further by UV/Vis/NIR or NIR/IR spectroelectrochemistry. The tight potential window of the three oxidation events (0 to $+1$ to $+2$ to $+4$) made it impossible to obtain separated spectra of the species owing to disproportionation and comproportionation reactions. However, careful oxidation from the neutral species to the radical cation $\mathbf{5}^+$ shows an intense broad band in the NIR centered at 4431 cm^{-1} ($\lambda = 2257$ nm; Figure 7).

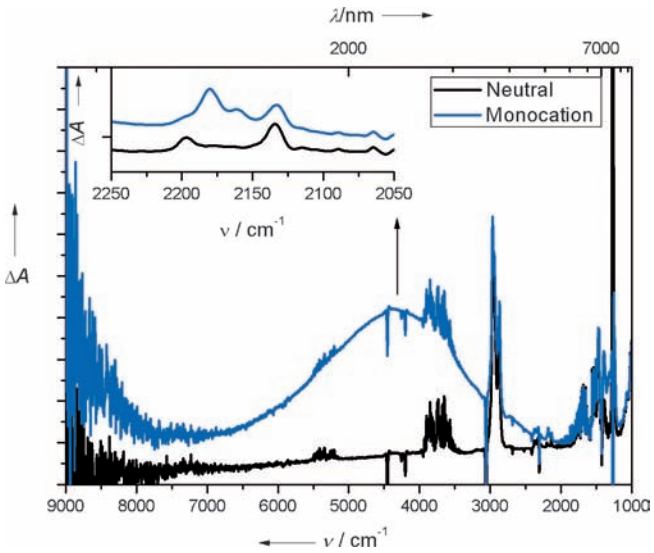

Figure 7. IR Spectra showing the oxidation of **5** to $\mathbf{5}^{+}$ (2.1×10^{-3} M in CH_2Cl_2 + 0.1 M $[NBu_4][PF_6]$).

This band implies electronic interaction between the TTFs through the RA spacer and is ascribed to an intervalence CT band.[15] Formation of the dication $\mathbf{5}^{2+}$ causes a lowering of this band, although it does not fully disappear because of dis/comproportionation. The dication $\mathbf{5}^{2+}$ exhibits a broad absorption at $\lambda = 930$ nm (Figure 8), which is characteristic of alkylthio-substituted TTF radical cations.[15b,16] Additional oxidation to the tetracation $\mathbf{5}^{4+}$ results in an absorption blue shift to $\lambda = 813$ nm. Reduction of **5** to the radical anion $\mathbf{5}^{-}$ causes the peak at $\lambda = 473$ nm to collapse while a strong absorption appears at $\lambda = 845$ nm (Figure 8) together with some lower-energy absorptions (see the Supporting Information). Neutral **5** shows very weak C≡C stretching bands at 2197 and 2134 cm^{-1} (see the Supporting Information). However, upon reduction to $\mathbf{5}^{-}$ they become far more intense and shift to lower energy (2167–1989 cm^{-1}). This weakening of

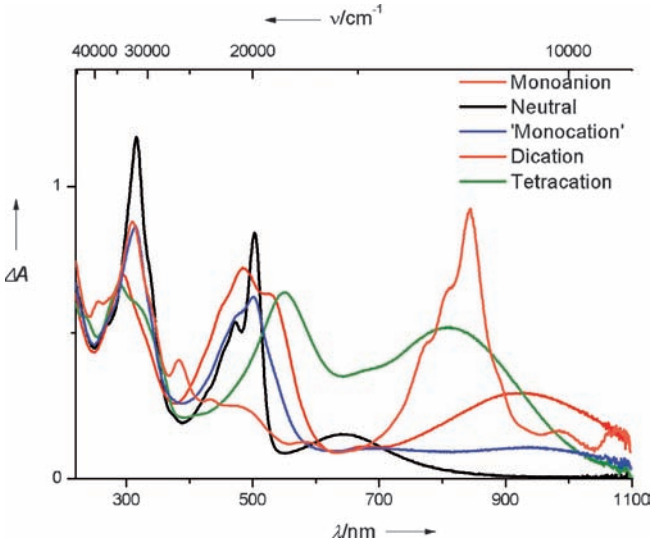

Figure 8. UV/Vis Absorption spectra of **5** in different charge states (0.6×10^{-3} M in CH_2Cl_2 + 0.1 M $[NBu_4][PF_6]$).

triple bonds indicates increased π-electron delocalization in the reduced species. The neutral species can be regenerated upon oxidation, that is, formation of the radical anion is chemically reversible.

The remarkably easy two-step reduction of the TTF/RA core agrees with a Wurster-type redox system and may indicate a gain in aromaticity in passing from **5** to $\mathbf{5}^{2-}$. To shed further light on this aspect, we performed a series of nucleus independent chemical shift (NICS) calculations, an index introduced by Schleyer and co-workers as a probe for aromaticity.[17] The values for compounds **1**, **2**, and **5**(4H) are shown in Table 1. In fact, both NICS(0) and more refined NICS indices clearly reveal a gain in aromaticity (more negative NICS), when proceeding from neutral RAs **2** and **5**(4H) to their corresponding dianions. While the values for $\mathbf{2}^{2-}$ and $\mathbf{5}(4H)^{2-}$ are rather similar, they are, nevertheless, less negative than those of the parent octadehydro[14]annulene (**1**).

Table 1: NICS values (B3LYP/6-31G(d)) for the octadehydro[14]annulene part of the planar, closed-shell RAs in comparison to **1**.

Compound	NICS(0)	$NICS(0)_{zz}$	NICS[π]	$NICS[\pi]_{zz}$
1	−16.8	−43.4	−21.0	−49.6
2	−0.7	+5.3	−6.2	−6.4
$\mathbf{2}^{2-}$	−10.9	−24.8	−16.1	−35.9
5(4H)	−0.7	+7.1	−7.1	−8.4
$\mathbf{5}(4H)^{2-}$	−8.7	−16.4	−15.4	−33.2

In conclusion, a cyclization involving four Sonogashira couplings has provided a fused Weitz/Wurster-type redox system, which formally gains Hückel aromaticity by either oxidation (6π-dithiolium units) or reduction (14π-octadehydroannulene unit). Moreover, the RA core allows a mixed valence TTF/RA/TTF^{+} structure. Substitution of the silyl groups with electron-withdrawing groups may enhance the electron affinity even further and is subject of future work. The six redox states (−2/−1/0/+1/+2/+4) characterized by electronic excitations covering altogether the UV/Vis/IR region could be attained electrochemically, thus making TTF/RAs interesting for future development of advanced electrochromic and electrically conducting materials.

Received: March 23, 2012
Revised: April 18, 2012
Published online: May 29, 2012

Keywords: alkynes · annulenes · aromaticity · redox chemistry · synthetic methods

[1] a) F. Mitzel, C. Boudon, J.-P. Gisselbrecht, P. Seiler, M. Gross, F. Diederich, *Helv. Chim. Acta* **2004**, *87*, 1130–1157; b) G. Chen, L. Wang, D. W. Thompson, Y. Zhao, *Org. Lett.* **2008**, *10*, 657–660; c) G. Chen, L. Dawe, L. Wang, Y. Zhao, *Org. Lett.* **2009**, *11*, 2736–2739; d) M. Gholami, M. N. Chaur, M. Wilde, M. J. Ferguson, R. McDonald, L. Echegoyen, R. R. Tykwinski, *Chem. Commun.* **2009**, 3038–3040; e) Y.-L. Wu, F. Bures, P. D.

Jarowski, W. B. Schweizer, C. Boudon, J.-P. Gisselbrecht, F. Diederich, *Chem. Eur. J.* **2010**, *16*, 9592 – 9605.
[2] H. Hopf, G. Maas, *Angew. Chem.* **1992**, *104*, 953 – 977; *Angew. Chem. Int. Ed. Engl.* **1992**, *31*, 931 – 954.
[3] E. L. Spitler, C. A. Johnson II, M. M. Haley, *Chem. Rev.* **2006**, *106*, 5344 – 5386.
[4] For a discussion of Wurster and Weitz systems, see: K. Deuchert, S. Hünig, *Angew. Chem.* **1978**, *90*, 927 – 938; *Angew. Chem. Int. Ed. Engl.* **1978**, *17*, 875 – 886.
[5] Y. Kuwatani, I. Ueda, *Angew. Chem.* **1995**, *107*, 2017 – 2019; *Angew. Chem. Int. Ed. Engl.* **1995**, *34*, 1892 – 1894.
[6] a) M. R. Bryce, *J. Mater. Chem.* **2000**, *10*, 589 – 598; b) J. L. Segura, N. Martín, *Angew. Chem.* **2001**, *113*, 1416 – 1455; *Angew. Chem. Int. Ed.* **2001**, *40*, 1372 – 1409; c) D. Jérome, *Chem. Rev.* **2004**, *104*, 5565 – 5591; d) D. Canevet, M. Sallé, G. X. Zhang, D. Zhang, D. Zhu, *Chem. Commun.* **2009**, 2245 – 2269; e) M. Hasegawa, M. Iyoda, *Chem. Soc. Rev.* **2010**, *39*, 2420 – 2427.
[7] For a computational study on the aromaticity of TTF cations, see: M. B. Nielsen, S. P. A. Sauer, *Chem. Phys. Lett.* **2008**, *453*, 136 – 139.
[8] J. Anthony, A. M. Boldi, Y. Rubin, M. Hobi, V. Gramlich, C. B. Knobler, P. Seiler, F. Diederich, *Helv. Chim. Acta* **1995**, *78*, 13 – 45.
[9] For synthesis, see the Supporting Information.
[10] Crystal data for **5**. $C_{76}H_{104}S_{12}Si_4$, $M_r = 1514.67$, triclinic, *P*-1, $a = 13.143(3)$, $b = 15.909(3)$, $c = 20.719(3)$ Å, $\alpha = 82.89(2)$, $\beta = 79.25(1)$, $\gamma = 82.90(2)°$, $V = 4200.9(14)$ Å^3, $T = 123$ K, $\mu(Mo_{K\alpha}) = 0.408$ mm^{-1}, $2\theta_{max} = 50.8°$, 83611 reflections measured, 14403 unique reflections ($R_{int} = 0.079$), 11539 observed reflections, $R1(I > 2\sigma(I)) = 0.047$, $wR2$(all data) = 0.105, $S = 1.10$. CCDC 871959 contains the supplementary crystallographic data for this paper. These data can be obtained free of charge from The Cambridge Crystallographic Data Centre via www.ccdc.cam.ac.uk/data_request/cif.
[11] a) J.-P. Gisselbrecht, N. N. P. Moonen, C. Boudon, M. B. Nielsen, F. Diederich, *Eur. J. Org. Chem.* **2004**, 2959 – 2972; b) M. B. Nielsen, F. Diederich, *Chem. Rev.* **2005**, *105*, 1837 – 1867.
[12] M. J. Frisch et al., *Gaussian 09*, Gaussian, Inc., Wallingford CT, **2010**. Complete reference: see the Supporting information.
[13] M. B. Robin, P. Day, *Adv. Inorg. Chem. Radiochem.* **1968**, *10*, 247 – 422.
[14] V. D. Parker, M. Tilset, O. Hammerich, *J. Am. Chem. Soc.* **1987**, *109*, 7905 – 7906.
[15] For other examples, see: a) K. Lahlil, A. Moradpour, C. Bowlas, F. Menou, P. Cassoux, J. Bonvoisin, J.-P. Launay, G. Dive, D. Dehareng, *J. Am. Chem. Soc.* **1995**, *117*, 9995 – 10002; b) H. Spanggaard, J. Prehn, M. B. Nielsen, E. Levillain, M. Allain, J. Becher, *J. Am. Chem. Soc.* **2000**, *122*, 9486 – 9494; c) J. Lyskawa, M. Sallé, J.-Y. Balandier, F. Le Derf, E. Levillain, M. Alain, P. Viel, S. Palacin, *Chem. Commun.* **2006**, 2233 – 2235; d) I. Aprahamian, J.-C. Olsen, A. Trabolsi, J. F. Stoddart, *Chem. Eur. J.* **2008**, *14*, 3889 – 3895; e) M. Hasegawa, Y. Kobayashi, K. Hara, H. Enozawa, M. Iyoda, *Heterocycles* **2009**, *77*, 837 – 842; f) A. Vacher, F. Barrière, T. Roisnel, L. Piekera-Sady, D. Lorcy, *Organometallics* **2011**, *30*, 3570 – 3578.
[16] a) Y. N. Kreicberga, O. Y. Neilands, *Zh. Org. Khim.* **1985**, *21*, 2009 – 2010; b) C. A. Christensen, L. M. Goldenberg, M. R. Bryce, J. Becher, *Chem. Commun.* **2000**, 331 – 332; c) V. Khodorkovsky, L. Shapiro, P. Krief, A. Shames, G. Mabon, A. Gorgues, M. Giffard, *Chem. Commun.* **2001**, 2736 – 2737.
[17] P. von R. Schleyer, C. Maerker, A. Drandfeld, H. Jiao, N. J. R. v. E. Hommes, *J. Am. Chem. Soc.* **1996**, *118*, 6317 – 6318.

